AD-A081 776 NAVAL RESEARCH LAB WASHINGTON DC F/G 4/1
THE PHYSICS OF THE PHOTODEPOSITION PHASE OF THE NRL MASTER CODE--ETC(U)
JAN 80 A W ALI
UNCLASSIFIED NRL-MR-4152 SBIE-AD-E000 376 NL

END
DATE
FILMED
4 80
DTIC

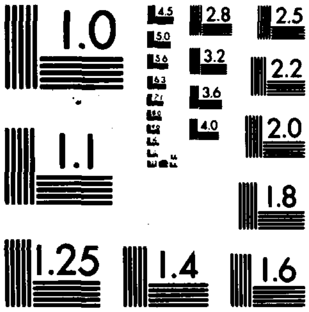

MICROCOPY RESOLUTION TEST CHART
NATIONAL BUREAU OF STANDARDS-1963-A

⑫ LEVEL III AD-E000 376

NRL Memorandum Report 4152

ADA081776

The Physics of the Photodeposition Phase of the NRL Master Code for the Disturbed E and F Regions

A. W. Ali

Plasma Physics Division

January 24, 1980

This work was sponsored by the Defense Nuclear Agency under Subtask S99QAXHD411,
work unit 15 and work unit title Reaction Rates Essential to Propagation.

DTIC
S ELECTE D
MAR 12 1980
B

NAVAL RESEARCH LABORATORY
Washington, D.C.

80 2 19 060

⑨ Memorandum rept.,

SECURITY CLASSIFICATION OF THIS PAGE (When Data Entered)

REPORT DOCUMENTATION PAGE

READ INSTRUCTIONS BEFORE COMPLETING FORM

1. REPORT NUMBER NRL Memorandum Report 4152 ✓	2. GOVT ACCESSION NO.	3. RECIPIENT'S CATALOG NUMBER
4. TITLE (and Subtitle) ⑥ THE PHYSICS OF THE PHOTODEPOSITION PHASE OF THE NRL MASTER CODE FOR THE DISTURBED E AND F REGIONS.		5. TYPE OF REPORT & PERIOD COVERED Interim report on a continuing NRL problem 6. PERFORMING ORG. REPORT NUMBER
7. AUTHOR(s) ⑩ A. W. Ali ⑭ NRL-MR-4152		8. CONTRACT OR GRANT NUMBER(s) ⑪ 24 Jan 80
9. PERFORMING ORGANIZATION NAME AND ADDRESS Naval Research Laboratory ✓ Washington, DC 20375		10. PROGRAM ELEMENT, PROJECT, TASK AREA & WORK UNIT NUMBERS NRL Problem 67-0851-0-0 DNA Subtask S99QAXHD411
11. CONTROLLING OFFICE NAME AND ADDRESS Defense Nuclear Agency Washington, DC 20305		12. REPORT DATE January 24, 1980 ⑫ 49 13. NUMBER OF PAGES 48
14. MONITORING AGENCY NAME & ADDRESS (if different from Controlling Office) ⑯ S99QAXH ⑰ D411		15. SECURITY CLASS. (of this report) UNCLASSIFIED 15a. DECLASSIFICATION/DOWNGRADING SCHEDULE

16. DISTRIBUTION STATEMENT (of this Report)

Approved for public release; distribution unlimited.

18 [illegible] / 19 [illegible] E[illegible] 376

17. DISTRIBUTION STATEMENT (of the abstract entered in Block 20, if different from Report)

18. SUPPLEMENTARY NOTES

This work was performed at the Naval Research Laboratory under the auspices of the Defense Nuclear Agency under subtask S99QAXHD411, work unit title Reaction Rates Essential to Propagation.

19. KEY WORDS (Continue on reverse side if necessary and identify by block number)

NRL Master Code
E & F Region
Photoionization

20. ABSTRACT (Continue on reverse side if necessary and identify by block number)

The physics of the revised photoionization phase for the NRL Master Code for the Disturbed E and F Region of the ionosphere is presented. The revision utilizes current total and partial photoionization cross sections.

DD FORM 1 JAN 73 1473 EDITION OF 1 NOV 65 IS OBSOLETE
S/N 0102-014-6601

SECURITY CLASSIFICATION OF THIS PAGE (When Data Entered)

251950

JOB

CONTENTS

THE PHYSICS OF THE PHOTODEPOSITION PHASE OF THE NRL MASTER CODE FOR THE DISTURBED E AND F REGIONS

I. INTRODUCTION

The fireball of a high altitude nuclear detonation emits a wide range of electromagnetic radiation. Among the emitted spectrum, the ultraviolet and the x-ray radiations dissociate and ionize a vast amount of the upper atmosphere and generate what is usually called the uv-fireball. The uv-fireball, as an ionized medium, impacts heavily on communication, radar, visible and infrared detectors and other systems of interest. Therefore, it is of considerable interest to predict the ionization and the deionization of the uv-fireball as accurately as possible. This requires adequate chemistry codes coupled to the hydro codes to describe the physics of the disturbed atmosphere in a self consistent manner. Adequate chemistry codes are generally simpler versions of more detailed chemistry codes which provide sufficient accuracy for the purposes of the desired calculations.

The NRL Master Code[1-3] is a detailed time dependent multispecies code which describes the evolution of ionization and deionization in the disturbed E and F regions of the ionospere. The calculations of the ionization and deionization are characterized by two time scales, the early time and the late time. The early time signifies the photodeposition phase and the late time commences with the termination of the ionizing radiation. During both of these phases a large number of reactions occur which determine the time histories of the species and

---

Note: Manuscript submitted November 13, 1979.

temperatures of interest. The most up to date version of this code has been reported recently[4] where the most appropritate and up to date reaction rates are incorporated.

The details of the photodeposition for the NRL Master Code was reported some time ago.[2,5] However, in view of current data on photoionization cross sections, a revision of the photodeposition phase of the NRL Master Code is warranted. This report, therefore, deals with the details of the photodeposition where a large number of ultraviolet and extreme ultraviolet spectral lines are considered.

II. PHOTODEPOSITION

The photodeposition of the NRL Master Code consists of the irradiation of the E and F regions by a large number of uv and euv radiation. This radiation consists of resonance and other strong uv lines emitted from oxygen and nitrogen atoms and their multiply ionized ions. A list of these spectral lines, their excitation energies[6] (the energy of the emitted photon), the species which emit them and their code designations is given in Table I.

Table I

Spectral Line (A)	Excitation Energy (eV)	Source of Emission	Code Designation
1303.50	9.50	O_I	L_1
1240.10	10.00	N_V	L_2
1199.90	10.33	N_I	L_3
1134.60	10.92	N_I	L_4
1085.10	11.43	N_{II}	L_5

Table I

Spectral Line (A)	Excitation Energy (eV)	Source of Emission	Code Designation
1033.80	11.99	O_{VI}	L_6
1026.60	12.10	O_I	L_7
990.98	12.51	N_{III}	L_8
989.50	12.54	O_I	L_9
916.34	13.53	N_{II}	L_{10}
878.50	14.11	O_I	L_{11}
834.50	14.86	O_{III}	L_{12}
833.80	14.87	O_{II}	L_{13}
811.40	15.28	O_I	L_{14}
789.36	15.71	O_{IV}	L_{15}
765.14	16.20	N_{IV}	L_{16}
764.01	16.23	N_{III}	L_{17}
703.36	17.63	O_{III}	L_{18}
685.71	18.08	N_{III}	L_{19}
671.48	18.46	N_{II}	L_{20}
644.99	19.22	N_{II}	L_{21}
629.73	19.69	O_V	L_{22}
609.35	20.35	O_{IV}	L_{23}
554.37	22.36	O_{IV}	L_{24}
539.40	22.99	O_{II}	L_{25}
533.67	23.23	N_{II}	L_{26}
529.68	23.41	N_{II}	L_{27}

Table I

Spectral Line (A)	Excitation Energy (eV)	Source of Emission	Code Designation
507.93	24.40	O_{III}	L_{28}
452.11	27.42	N_{III}	L_{29}
430.09	28.82	O_{II}	L_{30}
374.44	33.10	N_{III}	L_{31}
374.12	33.14	O_{III}	L_{32}
305.72	40.5	O_{III}	L_{33}
303.66	40.8	O_{III}	L_{34}
279.83	44.3	O_{IV}	L_{35}
247.20	50.2	N_{IV}	L_{36}
238.50	52.0	O_{IV}	L_{37}
209.28	59.2	N_{V}	L_{38}

These spectral lines irradiate N_2, O_2 and O which are the constituents of the ambient E and F regions and are considered to be mainly in their ground states. However, the irradiation time is generally long compared with the dissociative recombination times of N_2^+ and O_2^+. These recombinations form additional species e.g., N, $N(^2D)$, $N(^2p)$, $O(^1D)$, $O(^1S)$, etc., which have to be considered in a detailed photodeposition scheme.

The uv-fireball is a disturbed ionosphere with dimensions of hundreds of kilometers whose degree of ionization (or disturbance) at any point in space depends on the amount of absorbed radiation at that point. Thus the degree of ionization at any point in the uv-fireball depends directly on its distance from the radiation source (the fireball). This in principle requires a time and space dependent attenuation calculation of each spectral line emitted from the fireball. To illustrate, let I_λ (r,t) indicate the flux of a spectral line at time t a distance r from the fireball which can be considered as a point source. Then

$$I_\lambda(r,t) = \frac{1}{4\pi r^2} I_\lambda(r_0,t) \exp\left(-\sum_i \int_{r_0}^{r} N_i(r,t)\, \sigma_{t,\lambda}(N_i) dr\right) \tag{1}$$

where r_0 defines the coordinates of the fireball, $N_i(r,t)$ is the space and time dependent density of species, i, and $\sigma_{t,\lambda}(N_i)$ is the total absorption cross section of radiation at wavelength λ by species N_i. The exponential factor in equation (1) determines how far a given wavelength can be transmitted in any given direction before it is extinguished. The ion production rate from species N_i, can be given by

$$\frac{dN_i^+(r,t)}{dt} = \sum_\lambda I_\lambda(r,t)\, \sigma_{i,\lambda}(N_i)\, N_i(r,t) \tag{2}$$

where $\sigma_{i,\lambda}(N_i)$ is the photoionization cross section of species N_i due to radiation at wavelength, λ. On the other hand, the dissociation rate of molecular species is given by

$$\frac{dN_{2i}(r,t)}{dt} = -\sum_\lambda I_\lambda(r,t)\, \sigma_{d,\lambda}(N_{2i})\, N_{2i}(r,t) \tag{3}$$

where $\sigma_{d,\lambda}(N_{2i})$ is the photodissociation cross section of molecular species N_{2i} due to radiation at wavelength λ.

It is obvious from equation (3) that three quantities σ_t, σ_i and σ_d are required for a detailed photodeposition calculation. However, in addition to these, the final states of the ion, in the case of ionization, and that of the atom, in the case of dissociation, are very essential. In the case of ionization, one requires a knowledge of the partial photoionization cross sections at each wavelength, where generally each species has several ionization continuum. For example, for a 20 eV photon (∿620 Å) the nitrogen molecule cuould be in any one of its ionic states of $X^2\Sigma$, $A^2\pi$ and $B^2\Sigma$ whose ionization thresholds are at 15.58, 16.7 and 18.8 eV, respectively. The importance of the partial photoionization cross sections are obvious for several reasons: (1) They provide accurate photoelectron energies, (2) They provide the production rates for the excited states of the ions which are either metastable or radiatively allowed. If the state is metastable it could react faster with other species and hence affect the chemistry of the disturbed atmosphere. A good example in this case is the production of $O^+(^2D)$ which charge transfers with N_2 to produce N_2^+. The significance of this reaction is very clear for the disturbed upper atmosphere, where an atomic ion is converted into a molecular one which generally recombines with the free electron at a much faster rate. Furthermore, if the ionic state is a radiatively allowed state it could lose its energy by radiation, deexcitation by electrons, and by quenching with neutrals. These, depending on the density regime, provide fluorescence emission and may raise the kinetic energy of the electron and the neutral species. At shorter wavelengths dissociative ionization of the molecular species begin to contribute appreciably to the total ionization. This should be known accurately since they produce atomic ions whose recombination rates are not as fast as those of molecular ions. The final states of the atomic species due to photodissociation of the molecules provide much necessary information. These are the direct heating of the neutrals and the production of the metastable atomic states. The metastable states provide several interesting line emissions, contribute indirectly to neutral and electron heating and produce additional ionization due to photoionization by long wavelength radiation. Furthermore, atomic metastable states contribute to the formation of additional species through neutral reactions, e.g., $N(^2D) + O_2 \rightarrow NO + O$).

III. PHOTOABSORPTION AND PHOTOIONIZATION OF N_2

The photoabsorption and photoionization cross sections for N_2 in the wavelength range of interest have been measured previously (up to 1965) by many investigators.[8-12] These measurements and the measurement of others have been reviewed by Hudson.[13] This review also covers measurements of photoabsorption cross sections for other atmospheric molecules. While most of these measurements were concerned with the total photoionization cross section, some partial photoionization cross sections were reported by Blake and Carver[14] in 1967. However, recently, total[15] and partial[15,16] photoionization cross sections for N_2 have been reported over a wider range of wavelengths of interest. The agreement between these recent measurements are reasonably good, however, the agreement between them[15] and the older measurement[14] are poor.

In Table II we present the total photoabsorption, total and partial photoionization cross sections for the wavelength given in Table I. The branching ratios for the partial photoionization cross sections are shown in Figure 1 based on the measurements of Samson, et al.[15] The data for the partial dissociative ionization are from Wight, et al[17] as given in Reference 16. The sources for the data in Table II are indicated, however, the main source is due to the recent measurements of Samson, et al.[15]

Table II

Total Photoabsorption, Total and Partial Photoionization Cross Sections of N_2 in (Mb)

$\lambda(\mathring{A})$	σ_T	σ_i	$\sigma_i(X)$	$\sigma_i(A)$	$\sigma_i(B)$	$\sigma_i(\text{Diss})$	Ref.
1303.5	0	0					
1240.1	0	0					
1199.9	0	0					
1134.6	0	0					
1085.1	0	0					
1033.8	7.0×10^{-4}	0					18
1026.6	1.0×10^{-3}	0					18
990.98	0.10	0					18
989.50	0.16	0					18
916.34	0.2	0					9,19
878.50	0.35	0					9,19
834.50	3	0	0.0	0.0	0.0	0.0	8,9
833.80	5	0	0.0	0.0	0.0	0.0	8,9
811.40	22.0	0.0	0.0	0.0	0.0	0.0	9
789.36	22.7	10.2	10.2	0.0	0.0	0.0	18
765.14	85	65	65	0.0	0.0	0.0	18
764.01	13.5	9.3	9.3	0.0	0.0	0.0	18
703.36	25	24.2	8.0	16.0	0.0	0.0	15

Table II

Total Photoabsorption, Total and Partial Photoionization Cross Sections of N_2 in (Mb)

$\lambda(\mathring{A})$	σ_T	σ_i	$\sigma_i(X)$	$\sigma_i(A)$	$\sigma_i(B)$	$\sigma_i(\text{Diss})$	Ref.
685.71	24.9	24	7.6	16.4	0.0	0.0	18
671.48	34.3	33.3	10.5	22.8	0.0	0.0	15
644.99	24	24	7.1	13.8	2.9	0.0	15
629.73	23.75	23.75	7.2	13.7	2.9	0.0	15
609.35	23.75	23.75	7.3	13.7	2.7	0.0	15
554.37	24.25	24.25	8.7	13.1	2.5	0.0	15
539.40	25.4	25.4	9.4	13.5	2.5	0.0	15
533.67	25.4	25.4	9.9	13.2	2.3	0.0	15
529.68	25.4	25.4	9.9	13.2	2.3	0.0	15
507.93	24	24	9.7	12.4	1.9	0.0	15
452.11	22.5	22.5	10.2	9.76	1.55	1.0	15,17
430.09	22.5	22.5	10.0	10.0	1.5	0.87	15,17
373.36	17.5	17.5	7.5	7.1	1.3	1.50	15,17
374.12	17.5	17.5	7.5	7.1	1.3	1.5	15,17
305.72	11.50	11.50	3.2	4.8	1.0	2.5	15,17
303.66	11.5	11.5	3.2	4.8	1.0	2.5	15,17
279.83	10.5	10.5	2.4	4.4	1.2	2.5	15,17
247.20	9.5	9.5	2.2	3.7	0.95	3.3	15,17
238.50	9.5	9.5	2.2	3.7	0.95	3.3	15,17
209.28	7.0	7.0	1.2	2.6	0.7	2.5	15,17

With the data for the partial photoionization cross sections given in Table II one can claculate the average energy of the ejected photoelectron for each spectral line. These energies are given in Table III.

Table III

Average Photoelectron Energy From N_2 For Each Ionizing Wavelength

Wavelength	Designated Flux	Photoelectron Energy (eV)
1303.5	L_1	--
1240.1	L_2	--
1199.9	L_3	--
1134.6	L_4	--
1085.1	L_5	--
1033.8	L_6	--
1026.6	L_7	--
990.98	L_8	--
989.5	L_9	--
916.34	L_{10}	--
878.50	L_{11}	--
834.50	L_{12}	--
833.80	L_{13}	--
811.40	L_{14}	--
789.36	L_{15}	--
765.14	L_{16}	0.62
764.01	L_{17}	0.65
703.36	L_{18}	1.28
685.71	L_{19}	1.73
671.48	L_{20}	2.10
644.99	L_{21}	2.57
629.73	L_{22}	3.06
609.35	L_{23}	3.73
554.37	L_{24}	5.85
539.40	L_{25}	6.47
533.67	L_{26}	6.76

Table III (Continued)

Average Photoelectron Energy Ejected From N_2 For Each Ionizing Wavelength

Wavelength	Designated Flux	Photoelectron Ejected
529.68	L_{27}	6.94
507.93	L_{28}	7.94
452.11	L_{29}	10.74
430.09	L_{30}	12.09
374.44	L_{31}	16.10
374.12	L_{32}	16.12
305.72	L_{33}	22.20
303.66	L_{34}	22.52
279.83	L_{35}	22.55
247.20	L_{36}	32.92
238.50	L_{37}	34.8
209.28	L_{38}	39.42

However, one can simplify the calculations by regrouping of the spectral lines in a manner similar[20] to the solar ionization of the ionosphere. The regrouping depends on the degree of accuracy desired in the calculation and will be discussed later in this report.

IV. PHOTODISSOCIATION OF N_2

In Section II data were presented for the total photoabsorption cross section in N_2. The total and partial photoionization cross sections were also given including the relevent cross sections for the dissociative ionization. In this section a discussion is given on the photodissociation of N_2. There are several photodissociation limits [21] for N_2 where the products of the dissociation leave the nitrogen atoms in excited states. These dissociation limits, their threshold energies and the states of the dissociation products are given in Table IV, reproduced from Reference 21.

TABLE IV

Photodissociation Limits Of N_2

Limit	Products	Dissociation Energy (eV)	Wavelength (Å)
D_1	$^4S + {}^4S$	9.76	1270
D_2	$^2D + {}^4S$	12.14	1021
D_3	$^2P + {}^4S$	13.33	930
D_4	$^2D + {}^2D$	14.52	853
D_5	$^2P + {}^2D$	15.71	789
D_6	$^2P + {}^2P$	16.91	733
D_7	$^4P + {}^4S$	20.08	617

The photodissociation limits presented in Table IV produce states which are basically metastable, i.e. ^2D and ^2P and a radiatively allowed excited state ^4P which emits ultraviolet photons (~ 10.3 eV). These metastable states can, in principle, be photoionized by radiation of longer wavelengths compared to ionization from the ground state of the species.

There exist reliable measured photoabsorption and photoionization cross sections for N_2 (see Section II for references). However, the same cannot be said for photodissociation of N_2. In fact one may observe that no data is available for the simple photodissociation of N_2. However, some estimates can be made [21] from a knowledge of the measured total photoabsorption and photoionization cross sections. In Table V we present such an estimate based on the work of Reference 21, however, modified to conform with the average *total* absorption cross sections given in Table II. We also present in this table the products of the dissociation and the excess energy which goes into the kinetic energy of the neutrals.

Table V

N_2 Dissociation Cross Section (Mb)

The Dissociation Products and the Excess Energy Going into the Kinetic Energy of the Neutrals

	λ (Å)	σ_D(Mb)	Products	Excess Energy (eV)
L_9	989.50	0.08	$^4S + {}^2D$	0.42
L_{10}	916	0.14	$^4S + {}^2D$	1.41
L_{11}	878.5	0.30	$^4S + {}^2P$	0.78
L_{12}	834.5	1.4	$^4S + {}^2P$	1.53
L_{13}	833.8	1.5	$^4S + {}^2P$	1.54
L_{14}	811.4	1.2	$^4S + {}^2P$	1.95
L_{15}	789	2.2	$^2P + {}^2D$	0.0
L_{16}	765	1.8	$^2P + {}^2D$	0.49
L_{17}	764	1.8	$^2P + {}^2D$	0.52
L_{18}	703	0.8	$^2P + {}^2D$	1.92

V. PHOTOIONIZATION OF N

The photoionization cross section for the ground state of the nitrogen atom has been calculated by many workers using various theoretical methods[22-28]. Henry's results[23] agree reasonably well near threshold with experimental measurements of Comes and Elzer[27]. Reasonable agreement also prevails between the calculations of references 23, 24 and 26.

Of more interest, however, is the photoionization cross section of the ground state configuration of N i.e. N (^4S), N (^2D) and N (^2P). Such data has been presented by Henry[28] in a functional form fitted to the calculated value. The functional form is

$$\sigma_\lambda = \sigma_{th} \left[\alpha \left(\frac{\lambda}{\lambda_0} \right)^S + (1-\alpha) \left(\frac{\lambda}{\lambda_0} \right)^{S+1} \right] \times 10^{-18} \ (\mathrm{cm}^2) \quad (4)$$

where λ_0 is the threshold wavelength for the transition and α, S and σ_{th} are parameters whose values are given in Table VI.

Table VI

Photoionization Cross Section Parameters for N

Transition	S	α	σ_{th}
$N(^4S) \rightarrow N^+(^3P)$	2.0	4.287	11.42
$N(^2D) \rightarrow N^+(^3P)$	1.5	3.847	4.41
$N(^2D) \rightarrow N^+(^1D)$	2.0	4.826	5.02
$N(^2P) \rightarrow N^+(^3P)$	1.5	4.337	4.20
$N(^2P) \rightarrow N^+(^1D)$	2.0	5.112	2.87
$N(^2P) \rightarrow N^+(^1S)$	2.0	4.727	2.03

Using the parameters given in Table VI and equation (4), the photoionization cross sections for the ground state configuration of N are presented[29] in Figure 2 as a function of wavelength. Using this figure, the ionization cross sections for $N(^4S)$, $N(^2D)$ and $N(^2P)$ are presented in Tables VII (a) and VII (b) for the Set of ionizing radiation of Table I.

Table VII (a)

N Ground State Configuration

Photoionization Cross Sections (Mb) and the Energy of the Ejected Electron (eV)

Designated Flux	^4S-^3P/(ΔE)	^2D-^3P/(ΔE)	^2D-^1D/(ΔE)
L_4	--	--	--
L_5	--	--	--
L_6	--	--	--
L_7	--	--	--
L_8	--	4.6/0.35	--
L_9	--	4.6/0.38	--
L_{10}	--	4.8/1.37	--
L_{11}	--	4.9/1.96	5.0/0.05
L_{12}	11.4/0.33	5.0/2.7	5.3/0.80
L_{13}	11.4/0.34	5.0/2.71	5.3/0.81
L_{14}	11.7/0.75	5.0/3.12	5.6/1.22
L_{15}	11.9/1.18	5.0/3.55	5.6/1.65
L_{16}	11.9/1.67	4.9/4.04	5.7/2.14

Table VII (a) Continued
N Ground State Configuration
Photoionization Cross Sections (Mb) and the Energy of the Ejected Electron (eV)

Designated Flux	$^4S-^3P/(\Delta E)$	$^2D-^3P/(\Delta E)$	$^2D-^1D/(\Delta E)$
L_{17}	11.9/1.70	4.9/4.07	5.7/2.17
L_{18}	11.9/3.1	4.8/5.47	5.7/3.57
L_{19}	12.2/3.55	4.8/5.92	5.7/4.02
L_{20}	12.1/3.93	4.7/6.3	5.7/4.4
L_{21}	11.9/4.69	4.6/7.06	5.5/5.16
L_{22}	11.7/5.16	4.6/7.53	5.4/5.63
L_{23}	11.4/5.82	4.5/8.19	5.3/6.29
L_{24}	10.5/7.83	4.1/10.2	4.9/8.3
L_{25}	10.3/8.46	4.1/10.83	4.6/8.93
L_{26}	10.2/8.7	4.0/11.07	4.6/9.17
L_{27}	10.0/8.88	4.0/11.25	4.6/9.35
L_{28}	9.6/9.87	3.8/12.24	4.4/10.34
L_{29}	8.4/12.89	3.4/15.26	3.8/13.36
L_{30}	7.8/14.29	3.2/16.66	3.6/14.76

Table VII (a) Continued

N Ground State Configuration

Photoionization Cross Sections (Mb) and the Energy of the Ejected Electron (eV)

Designated Flux	$^4S-^3P/(\Delta E)$	$^2D-^3P/(\Delta E)$	$^2D-^1D/(\Delta E)$
L_{31}	6.4/18.57	2.8/20.94	3.0/19.04
L_{32}	6.4/18.61	2.8/20.98	3.0/19.08
L_{33}	4.7/25.97	2.1/28.34	2.1/26.44
L_{34}	4.7/26.27	2.1/28.64	2.1/26.74
L_{35}	4.0/29.77	1.8/32.14	1.8/30.24
L_{36}	3.3/35.67	1.5/38.04	1.5/36.14
L_{37}	3.2/37.47	1.4/39.84	1.4/37.94
L_{38}	2.5/44.67	1.0/47.04	1.0/45.14

Table VII (b)

N Ground State Configuration

Photoionization Cross Sections (Mb) and the Energy of the Ejected Electron (eV)

Designated Flux	$^2P-^3P/(\Delta E)$	$^2P-^1D/(\Delta E)$	$^2P-^1S/(\Delta E)$
L_4	--	--	--
L_5	4.5/0.47	--	--
L_6	4.7/1.03	--	--
L_7	4.7/1.14	--	--
L_8	4.8/1.55	--	--
L_9	4.8/1.58	--	--
L_{10}	5.0/2.57	3.1/0.67	--
L_{11}	5.1/3.15	3.2/1.25	--
L_{12}	5.0/3.90	3.3/2.00	--
L_{13}	5.0/3.91	3.3/2.01	--
L_{14}	5.0/4.32	3.3/2.42	2.2/0.27
L_{15}	4.9/4.75	3.3/2.85	2.2/0.70
L_{16}	4.9/5.24	3.3/3.34	2.2/1.19

Table VII (b) Continued

N Ground State Configuration

Photoionization Cross Sections (Mb) and the Energy of the Ejected Electron (eV)

Designated Flux	$^2P-^3P/(\Delta E)$	$^2P-^1D/(\Delta E)$	$^2P-^1S/(\Delta E)$
L_{17}	4.9/5.27	3.3/3.37	2.2/1.22
L_{18}	4.8/6.67	3.2/4.77	2.3/2.62
L_{19}	4.8/7.12	3.2/5.22	2.3/3.07
L_{20}	4.8/7.5	3.1/5.60	2.3/3.45
L_{21}	4.5/8.26	3.0/6.36	2.2/4.21
L_{22}	4.4/8.73	3.0/6.83	2.2/4.68
L_{23}	4.2/9.39	2.9/7.49	2.2/5.34
L_{24}	3.9/11.4	2.6/9.5	2.1/7.35
L_{25}	3.8/12.03	2.5/10.13	1.9/7.98
L_{26}	3.8/12.27	2.5/10.37	1.9/8.22
L_{27}	3.8/12.45	2.5/10.55	1.9/8.4

Table VII (b) Continued

N Ground State Configuration

Photoionization Cross Sections (Mb) and the Energy of the Ejected Electron (eV)

Designated Flux	$^2P-^3P/(\Delta E)$	$^2P-^1D/(\Delta E)$	$^2P-^1S/(\Delta E)$
L_{28}	3.6/13.44	2.3/11.54	1.8/9.39
L_{29}	3.3/16.96	2.0/14.56	1.6/12.41
L_{30}	3.1/17.86	1.8/15.96	1.5/13.81
L_{31}	2.7/22.14	1.5/20.24	1.2/18.09
L_{32}	2.7/22.18	1.5/20.28	1.2/18.13
L_{33}	2.1/29.54	1.0/27.64	0.8/25.49
L_{34}	2.1/29.84	1.0/27.94	0.8/25.79
L_{35}	1.9/33.34	0.9/31.44	0.7/29.29
L_{36}	1.6/39.24	0.7/37.34	0.6/35.19
L_{37}	1.6/41.04	0.7/39.14	0.6/36.99
L_{38}	1.2/48.24	0.5/46.34	0.4/44.19

VI. Photoionization of O

A recent measurement[30] of the photoionization cross section of atomic oxygen in the wavelength region of 900 - 760 Å gives results in close agreements with the measured values of Cairns and Sampson[31]. More rigorous and recent theortical calculations[24,28,34] predict results in reasonable accord with these measurements. However, early theortical calculations[34,35] have predicted results, near ionization threshold, which are lower by a factor of 2.

For a detailed photodeposition, one requires photoionization data for the ground state configuration for which no experimental data is available. However, theoretical calculations[28,34] exist and we shall utilize the results of Henry[28] by multiplying them by a factor of 1.6 to bring them into accord with the experimental data, especially for the transition ^3P - ^4S. Figure 3 presents the photoionization cross sections of $O(^3P)$, $O(^1D)$ and $O(^1S)$ calculated using equation (4) whose parameters relevent[28] to oxygen are given in Table VIII.

Table VIII

Photoionization Cross Section Parameters for O

Transition	S	α	σ_{th}
$O(^3P) \rightarrow O^+ (^4S)$	1.0	2.661	2.94
$O(^3P) \rightarrow O^+ (^2D)$	1.5	4.378	3.85
$O(^3P) \rightarrow O^+ (^2P)$	1.5	4.311	2.26
$O(^1D) \rightarrow O^+ (^2D)$	1.5	6.829	4.64
$O(^1D) \rightarrow O^+ (^2P)$	1.5	4.8	1.95
$O(^1S) \rightarrow O^+ (^2P)$	1.5	5.124	7.65

Tables IX a and IX b present the relevent photoionization cross section for the set of ionizing radiation of Table I. The energy of the ejected electrons are also given in Tables IX a and IX b.

Table IX (a)

O Ground State Configuration

Photoionization Cross Sections (Mb) and the Energy of the Ejected Electron (eV)

Designated Flux	$^3P \rightarrow {}^4S/(\Delta E)$	$^3P \rightarrow {}^2D/(\Delta E)$	$^3P \rightarrow {}^2P/(\Delta E)$
L_{11}	4.8/0.5	--	--
L_{12}	4.8/1.25	--	--
L_{13}	4.8/1.26	--	--
L_{14}	4.9/1.67	--	--
L_{15}	4.9/2.1	--	--
L_{16}	4.9/2.59	--	--
L_{17}	4.9/2.62	--	--
L_{18}	4.9/4.02	4.1/0.7	--
L_{19}	5.0/4.47	4.2/1.15	--
L_{20}	5.0/4.85	4.2/1.53	--
L_{21}	5.0/5.61	4.5/2.29	2.3/0.59
L_{22}	5.0/6.08	4.6/2.76	2.4/1.06
L_{23}	4.8/6.74	4.7/3.42	2.6/1.72

Table IX (a) Continued

O Ground State Configuration

Photoionization Cross Sections (Mb) and the Energy of the Ejected Electron (eV)

Designated Flux	$^3P \to {}^4S/(\Delta E)$	$^3P \to {}^2D/(\Delta E)$	$^3P \to {}^2P/(\Delta E)$
L_{24}	4.7/8.75	4.5/5.43	2.7/3.73
L_{25}	4.7/9.38	4.5/6.10	2.7/4.36
L_{26}	4.6/9.62	4.5/6.30	2.7/4.6
L_{27}	4.6/9.8	4.5/6.48	2.7/4.78
L_{28}	4.5/10.79	4.5/7.47	2.7/5.77
L_{29}	4.5/13.81	4.3/10.49	2.6/8.79
L_{30}	4.4/15.21	4.2/11.89	2.5/10.19
L_{31}	3.8/19.49	3.7/16.17	2.2/14.47
L_{32}	3.8/19.53	3.7/16.21	2.2/14.51
L_{33}	3.4/26.89	2.9/23.57	1.8/21.87
L_{34}	3.4/27.19	2.9/23.87	1.8/22.17
L_{35}	3.2/30.69	2.7/27.37	1.7/25.67

Table IX (a) Continued

O Ground State Configuration

Photoionization Cross Sections (Mb) and the Energy of the Ejected Electron (eV)

Designated Flux	$^3P \rightarrow {}^4S/(\Delta E)$	$^3P \rightarrow {}^2D/(\Delta E)$	$^3P \rightarrow {}^2P/(\Delta E)$
L_{36}	2.9/36.59	2.5/33.27	1.6/31.57
L_{37}	2.6/38.39	2.5/35.07	1.5/33.37
L_{38}	2.6/45.59	1.9/42.27	1.4/40.57

Table IX (b)

O Ground State Configuration

Photoionization Cross Sections (Mb) and the Energy of the Ejected Electron (eV)

Designated Flux	$^1D \to {}^2D/(\Delta E)$	$^1D \to {}^2P/(\Delta E)$	$^1S \to {}^2P/(\Delta E)$
L_{11}	--	--	--
L_{12}	--	--	8.2/.41
L_{13}	--	--	8.2/0.42
L_{14}	5.3/0.31	--	8.5/0.84
L_{15}	6.0/0.74	--	9.0/1.27
L_{16}	6.4/1.23	--	9.2/1.76
L_{17}	6.4/1.26	--	9.2/1.79
L_{18}	6.8/2.66	2.2/0.96	9.8/3.19
L_{19}	7.2/3.11	2.3/1.41	10.1/3.64
L_{20}	7.3/3.49	2.3/1.79	10.1/4.02
L_{21}	7.4/4.25	2.3/2.55	10.1/4.78
L_{22}	7.4/4.72	2.3/3.02	10.1/5.25
L_{23}	7.4/5.38	2.4/3.68	10.0/5.91

Table IX (b) Continued

O Ground State Configuration

Photoionization Cross Sections (Mb) and the Energy of the Ejected Electron (eV)

Designated Flux	$^1D \to {}^2D/(\Delta E)$	$^1D \to {}^2P/(\Delta E)$	$^1S \to {}^2P/(\Delta E)$
L_{24}	7.4/7.39	2.4/5.69	9.7/7.92
L_{25}	7.3/8.02	2.4/6.32	9.7/8.55
L_{26}	7.3/8.26	2.4/6.56	9.6/8.79
L_{27}	7.3/8.44	2.4/6.74	9.6/8.97
L_{28}	7.2/9.45	2.4/7.75	9.4/9.98
L_{29}	6.7/12.45	2.3/10.75	8.5/12.98
L_{30}	6.3/13.31	2.3/11.61	8.3/13.84
L_{31}	5.8/18.13	2.1/16.43	7.5/18.66
L_{32}	5.8/18.17	2.1/16.47	7.5/18.70
L_{33}	4.7/25.53	1.8/23.83	6.2/26.06
L_{34}	4.7/25.83	1.8/24.13	6.2/26.36
L_{35}	4.2/29.33	1.6/27.63	5.3/29.86

Table IX (b) Continued

O Ground State Configuration

Photoionization Cross Sections (Mb) and the Energy of the Ejected Electron (eV)

Designated Flux	$^1D \to {}^2D/(\Delta E)$	$^1D \to {}^2P/(\Delta E)$	$^1S \to {}^2P/(\Delta E)$
L_{36}	3.8/35.23	1.5/33.53	4.4/35.76
L_{37}	3.7/37.03	1.5/35.33	4.4/37.56
L_{38}	2.8/44.23	1.1/42.53	3.3/44.76

VII. Photoabsorption and Photoionization of O_2

The absorption cross sections for molecular oxygen have been measured below 1300 Å by many workers[9-11,19,35] and the data have been reviewed by Hudson[13]. Above 1300 Å the absorption cross section have been measured by Watanabe, et al,[37] and Metzger and Cook.[38] Partial photoionization cross sections are available,[14,39] however, over a limited range of wavelength. Dissociative photoionization cross sections have also been measured[40], again, over a limited range. Using these data, the total photoabsorption, photoionization and partial photoionization cross section are presented in Table X where the source of the data is also indicated. For regions of wavelength where no measurement is available estimates are provided. The photoionization to different continuum states of O_2 e.g. $X^2\pi$, $a^4\pi$, $A^2\pi$, $b^4\Sigma$ and dissociative ionization are considered.

Table X

Total Photoabsorption, Total and Partial Photoionization Cross Sections in O_2(Mb)

λ	σ_T	σ_i	$\sigma_{i(X)}$	$\sigma_{i(a)}$	$\sigma_{i(A)}$	$\sigma_{i(b)}$	$\sigma_{i(Diss.)}$	Ref.
1303.5	0.5	--	--	--	--	--	--	37,38
1240.1	0.2	--	--	--	--	--	--	19,38
1199.9	1.6	--	--	--	--	--	--	19,38
1134.6	1.0	--	--	--	--	--	--	19,38
1085.1	1.0	--	--	--	--	--	--	19
1033.8	0.9	--	--	--	--	--	--	10
1026.6	1.5	0.96	--	--	--	--	--	10
990.98	3.3	2.1	--	--	--	--	--	35
989.5	1.5	1.0	--	--	--	--	--	35
916.34	4.2	2.7	--	--	--	--	--	35
878.50	5.9	3.7	--	--	--	--	--	35
834.50	10.7	4.4	--	--	--	--	--	35
833.80	12.0	3.7	--	--	--	--	--	35
811.40	38.9	14.8	--	--	--	--	--	35
789.36	25.9	11.1	--	--	--	--	--	35
765.14	23.0	12.4	11.2	1.2	--	--	--	10
764.01	19.6	11.3	10.2	1.1	--	--	--	35
703.36	28.3	22.2	12.5	6.7	3.0	--	--	35
685.71	22.3	22.3	8.0	9.5	4.8	--	--	35

Table X Continued

Total Photoabsorption, Total and Partial Photoionization Cross Sections in O_2(Mb)

λ	σ_T	σ_i	$\sigma_{i(X)}$	$\sigma_{i(a)}$	$\sigma_{i(A)}$	$\sigma_{i(b)}$	$\sigma_{i(Diss.)}$	Ref.
671.48	22.2	22.2	4.4	6.2	3.1	8.5	--	35
644.99	24.1	23.10	4.6	5.3	3.0	9.9	0.3	35
629.73	32.3	31.2	6.8	7.0	3.5	13.1	0.8	35
609.35	26.3	25.5	6.8	6.1	2.9	8.4	1.3	35
554.37	26.4	25.6	5.4	5.2	4.5	6.4	4.0	35
539.4	26.4	25.6	5.2	5.1	4.6	6.4	4.3	35
533.67	24.5	23.7	3.3	5.0	4.0	7.1	4.3	35
529.68	24.5	23.7	3.3	5.0	4.0	7.1	4.3	35
507.93	23.1	22.4	3.3	4.0	4.0	7.1	4.0	10
452.11	20.8	20.8	3.2	4.5	4.5	6.6	2.0	35
430.09	17.8	17.8	3.0	3.4	4.4	6.0	1.0	10
373.36	18.0	18.0	3.0	4.1	4.4	6.0	0.5	10
374.12	18.0	18.0	3.0	4.1	4.4	6.0	0.5	10,13
305.72	16.4	16.4	2.9	3.0	4.0	6.0	0.5	10,13
303.66	16.6	16.6	2.9	3.0	4.2	6.0	0.5	10,13
279.83	14.8	14.8	2.8	2.2	3.3	6.0	0.5	10,13
247.20	12.0	12.0	2.7	2.2	2.6	4.0	0.5	10,13
238.50	11.0	11.0	2.7	1.8	2.0	4.0	0.5	10,13
209.28	9.0	9.0	2.5	1.5	2.0	3.0	0.0	10,13

The average energy of the ejected photoelectron can be calculated for each ionizing wavelength knowing the ionization threshold and the photoionization cross section. However, in O_2 the photoionization continuum lead to four discrete ionic states in addition to the dissociative ionization. These states are $X^2\pi$, $a^4\pi$, $A^2\pi$ and $b^4\Sigma$ whose ionization thresholds are 12.06, 16.1, 16.8 and 18.2 eV respectively. The $A^2\pi$ and $b^4\Sigma$ states are coupled radiatively to $X^2\pi$ and $a^4\pi$ states, where the $X^2\pi$ state is the ground state of the molecular ion and $a^4\pi$ is an excited and a metastable state. Thus, for the purposes of ionization one can consider the molecular ions to be in $X^2\pi$ and $a^4\pi$ states only and calculate the average photoelectron energy by utilizing the detailed data of Table XI.

Table XI

Effective Photoionization Cross Section of O_2 (Mb)
And the Average Energy of the Ejected Electron
For Each Ionizing Wavelength

Wavelength	Designated Flux	σ(X)	σ(a)	σ(di)	ΔE*(eV)
1303.5	L_1	--	--	--	--
1240.1	L_2	--	--	--	--
1199.9	L_3	--	--	--	--
1134.6	L_4	--	--	--	--
1085.1	L_5	--	--	--	--
1033.8	L_6	--	--	--	--
1026.6	L_7	0.90	0.0	--	0.04
990.98	L_8	2.1	0.0	--	0.45

Table XI Continued

Effective Photoionization Cross Section of O_2 And the Average Energy of the Ejected Electron For Each Ionizing Wavelength

Wavelength	Designated Flux	$\sigma(X)$	$\sigma(a)$	$\sigma(di)$	ΔE (eV)
989.5	L_9	1.0	0.0	--	0.48
916.34	L_{10}	2.7	0.0	--	1.47
878.50	L_{11}	3.7	0.0	--	2.05
834.50	L_{12}	4.4	0.0	--	2.8
833.80	L_{13}	3.7	0.0	--	2.81
811.40	L_{14}	14.8	0.0	--	3.22
789.36	L_{15}	11.1	0.0	--	3.65
765.14	L_{16}	11.2	1.2	--	4.14 - 0.1
764.01	L_{17}	10.2	1.1	--	4.17 - 0.13
703.36	L_{18}	15.5	6.7	--	4.65 - 1.53
685.71	L_{19}	12.8	9.5	--	4.24 - 1.98
671.48	L_{20}	7.5	14.7	--	4.44 - 1.14
644.99	L_{21}	7.6	15.2	0.3	5.29 - 1.75 - 0.51
629.73	L_{22}	10.3	20.1	0.8	6.02 - 3.63 - 0.98
609.35	L_{23}	9.7	14.5	1.3	6.87 - 3.03 - 1.64
554.37	L_{24}	10.0	11.6	4.0	8.12 - 5.10 - 3.65
539.40	L_{25}	9.8	11.5	4.3	8.70 - 5.72 - 4.28
533.67	L_{26}	7.3	12.1	4.3	8.57 - 5.89 - 4.52
529.68	L_{27}	7.3	12.1	4.3	8.75 - 6.07 - 4.7
507.93	L_{28}	7.3	11.1	4.0	9.74 - 6.95 - 5.69
452.11	L_{29}	7.7	11.1	2.0	12.58 - 10.07 - 8.71

Table XI Continued

Effective Photoionization Cross Section of O_2
And the Average Energy of the Ejected Electron
For Each Ionizing Wavelength

Wavelength	Designated Flux	σ(X)	σ(a)	σ(di)	ΔE(eV)
430.09	L_{30}	7.7	9.4	1.0	13.40 - 11.38 - 10.11
374.44	L_{31}	7.7	10.1	0.5	17.51 - 15.75 - 14.39
374.12	L_{32}	7.7	10.1	0.5	17.51 - 15.75 - 14.43
305.72	L_{33}	6.9	9.0	0.5	25.69 - 23.00 - 21.79
303.66	L_{34}	7.1	9.0	0.5	25.93 - 23.3 - 22.09
279.83	L_{35}	6.1	8.2	0.5	29.67 - 26.66 - 25.59
247.20	L_{36}	5.3	6.2	0.5	35.8 - 32.74 - 31.49
238.50	L_{37}	4.7	5.8	0.5	37.92 - 34.45 - 33.29
209.28	L_{38}	4.7	5.8	0.0	45.1 - 41.65 - 40.49

In this Table the energy of the ejected electron is given in three columns to correspond from left to the ionization limits σ(X), σ(a) and σ (di), respectively.

VIII. PHOTODISSOCIATION OF O_2

The oxygen molecule has many photodissociation limits where the products of the dissociation are oxygen atoms in excited states. The lowest dissociation limit is at 5.1 eV and the dissociation products are two atoms which are in the ground state. However, since we are interested in the photoabsorption at and below 1303 Å the dissociation limits of interest begin with the product of $O(^3P) + O(^1S)$. Table XII presents the dissociation limits of interest, their threshold energy and the products of the dissociations.

Table XII

O_2 Dissociation Limits and Dissociation Products

Energy Threshold (eV)	Wavelength (Å)	Dissociation Products
9.31	1331	$^3P + {}^1S$
11.27	1100	$^1D + {}^1S$
13.51	918	$^1S + {}^1S$
14.20	869	$^3P + {}^5S$
14.64	847	$^3P + {}^3S$
15.86	782	$^3P + {}^5P$
16.10	770	$^3P + {}^3P$
16.55	749	$^1D + {}^3S$
16.95	731	$^3P + {}^5S$
17.05	727	$^3P + {}^3S$
17.19	721	$^3P + {}^5D$
17.20	721	$^3P + {}^3D$

The dissociation cross section for O_2 from 1303 to 918 Å are taken from Tables XI (a,b) where we consider the total absorption to lead to dissociation in the absence of ionization. From ionization threshold to 918 Å we take the difference between total absorption and ionization to lead to dissociation. For wavelengths below 918 Å we utilize the measured values of Matsunaga and Watanabe[35] down to a wavelength where the ionization efficiency becomes 100%. Using these data, the dissociation cross sections of O_2 and the states of the dissociation products along with the excess energy which goes into the kinetic energy of the neutral particles are presented in Table XIII.

Table XIII

O_2 Dissociation Cross Section (Mb), the Dissociation Products and the Excess Energy Going into the Kinetic Energy of the Neutrals

Designated Flux	σ_d	Products	Excess Energy (eV)
L_1	0.5	$^3P + {}^1S$	0.19
L_2	0.2	$^3P + {}^1S$	0.69
L_3	1.6	$^3P + {}^1S$	1.02
L_4	1.0	$^3P + {}^1S$	1.61
L_5	1.0	$^1D + {}^1S$	0.16
L_6	0.9	$^1D + {}^1S$	0.72
L_7	0.5	$^1D + {}^1S$	0.83
L_8	1.2	$^1D + {}^1S$	1.24
L_9	0.5	$^1D + {}^1S$	1.27
L_{10}	0.5	$^1S + {}^1S$	0.02
L_{11}	2.3	$^1S + {}^1S$	0.6

Table XIII Continued

O_2 Dissociation Cross Section (Mb), the
Dissociation Products and the Excess Energy
Going into the Kinetic Energy of the Neutrals

Designated Flux	σ_d	Products	Excess Energy (eV)
L_{12}	5.5	$^3P + {}^3S^*({}^3P)^{(*)}$	0.22
L_{13}	5.5	$^3P + {}^3S^*({}^3P)$	0.23
L_{14}	10.2	$^3P + {}^3S^*({}^3P)$	0.64
L_{15}	9.2	$^3P + {}^3S^*({}^3P)$	1.07
L_{16}	8.1	$^3P + {}^3P^*({}^3P)$	0.1
L_{17}	8.1	$^3P + {}^3P^*({}^3P)$	0.13
L_{18}	2.7	$^3P + {}^3S^*({}^3P)$	0.58

(*) The state in the bracket is the final state since the original product is radiative and cascades to the ground state after emitting it excitation energy.

References

1. A. W. Ali, "Electron Pressure Profile in the F-Layer UV-Fireball", Plasma Dynamics Tech., Note 20, Plasma Physics Division, NRL(1969)
2. A. W. Ali, "The Chemistry and the Rate Coefficients of the F-Layer UV-Fireball", Plasma Dynamics Tech. Note 24 (1970).
3. A. W. Ali, "The Physics and Chemistry of Two NRL Codes for the Disturbed E and F Regions", NRL Report No. 7578(1973).
4. A. W. Ali, "The Physics and the Chemistry of NRL Master Code for The Disturbed E and F Regions", NRL Memorandum Report No.3732(1978).
5. A. W. Ali and E. B. Hyman, "Summary of NRL Results for First Chemistry Benchmark Meeting", RAND Corp., BO-31 March 1971(May 1971).
6. W. L. Wiese, M. W. Smith and B. M. Glennon, "Atomic Transition Probabilities", NSRDS-NBS 4, Vol. 1.(1966)
7. See for example, F. R. Gilmore "Potential Energy Curves for N_2, NO, O_2 and Corresponding Ions", RAND Corp. Memorandum RM-4034-1-PR (1966).
8. R. E. Huffman, Y. Tanaka and J. C. Larrabee, J. Chem. Phys. 39, 910 (1963).
9. G. R. Cook and P. H. Metzger, J. Chem. Phys. 41, 321 (1964).
10. J. A. R. Samson and R. B. Cairns, J. Geophys. Res. 69, 4583 (1964).
11. J. A. R. Samson and R. B. Cairns, J. Opt. Soc. Amer. 55, 1035 (1965).
12. K. Watanabe and F. F. Marmo, J. Chem. Phys. 25, 965 (1956).
13. R. D. Hudson, Rev. Geophys. Space Phys. 9, 305 (1971) and refer-references therein.
14. A. J. Blake and J. H. Carver, J. Chem. Phys. 47, 1038 (1967).

15. J. A. R. Samson, G. N. Haddad and J. L. Gardner, J. Phys. B: Atom Mol. Phys., 10, 1749 (1977).

16. E. W. Plummer, T. Gustafsson, W. Gudat and D. E. Eastman, Phys. Rev. A. 15, 2339 (1977).

17. G. R. Wight, M. J. Van der Wiel and C. E. Brion, J. Phys. B: Atom Mol. Phys. 9, 675 (1976).

18. G. V. Marr, "Photoionization Processes in Gases", Academic Press, New York (1967).

19. K. Watanabe, Adv. Geophys. 2, 153 (1958).

20. A. W. Ali and P. C. Kepple, "Solar Ionization Rates For The Ionosphere E, F and D Regions", NRL Report 7598 (1973).

21. G. R. Cook, M. Ogawa and R. W. Carlson, J. Geophys. Res. 78, 1663 (1973).

22. R. J. W. Henry and L. Lipsky, Phys. Rev. 153, 51 (1967)

23. R. J. W. Henry, J. Chem. Phys. 48, 3635 (1968).

24. G. M. Thomas and T. M. Helliwell, JQSRT, 10, 423 (1970).

25. A. Dalgarno, R. J. W. Henry and A. L. Stewart, Planet Space Sci., 12, 235 (1964)

26 S. Ormonde and M. J. Conneely, Q-SI-TR-70-69, Dec. (1970).

27. F. J. Comes and A. Elzer, Phys. Letters 25A, 334 (1967).

28. R. J. W. Henry, Astrophy. J. 161, 1153 (1970).

29. A. W. Ali, "Photoionization Cross Sections of O and N Atoms and Their Low Lying Metastable States", NRL, Plasma Dynamics Technical Note 32 (1971).

30. J. L. Kohl, G. P. Lafyatis, H. P. Palenius and W. H. Parkinson, Phys. Rev. A 18, 571 (1978).

31. R. B. Cairns and J. A. R. Sampson, Phys. Rev. 139, A 1403 (1965).

32. K. T. Taylor and P. G. Burke, J. Phys. B 9, L 353 (1976).

33. A. K. Pradhan and H. E. Saraph, J. Phys. B 10, 3365 (1977).

34. A. Dalgarno, R. J. W. Henry and A. I. Stewart, Planet Space Sci., 12, 235 (1964).

35. F. M. Matsuraga and K. Watanabe, Sci. Light. 16, 31 (1967).

36. R. E. Huffman, J. C. Larrabe and Y. Tanaka, J. Chem. Phys. 40, 356 (1964).

37. K. E. Watanabe, E. C. Y Inn and M. Zelikoff, J. Chem. Phys. 21, 1026 (1953).

38. P. H. Metzger, and G. R. Cook, JQRST, 4, 107 (1964).

39. A. J. Blake and J. H. Carver, Phys. Lett. 19, 387 (1965).

40. F. J. Comes, F. Speier and A. Elzer, Z.Natureforsch, 23A, 125, 1968.

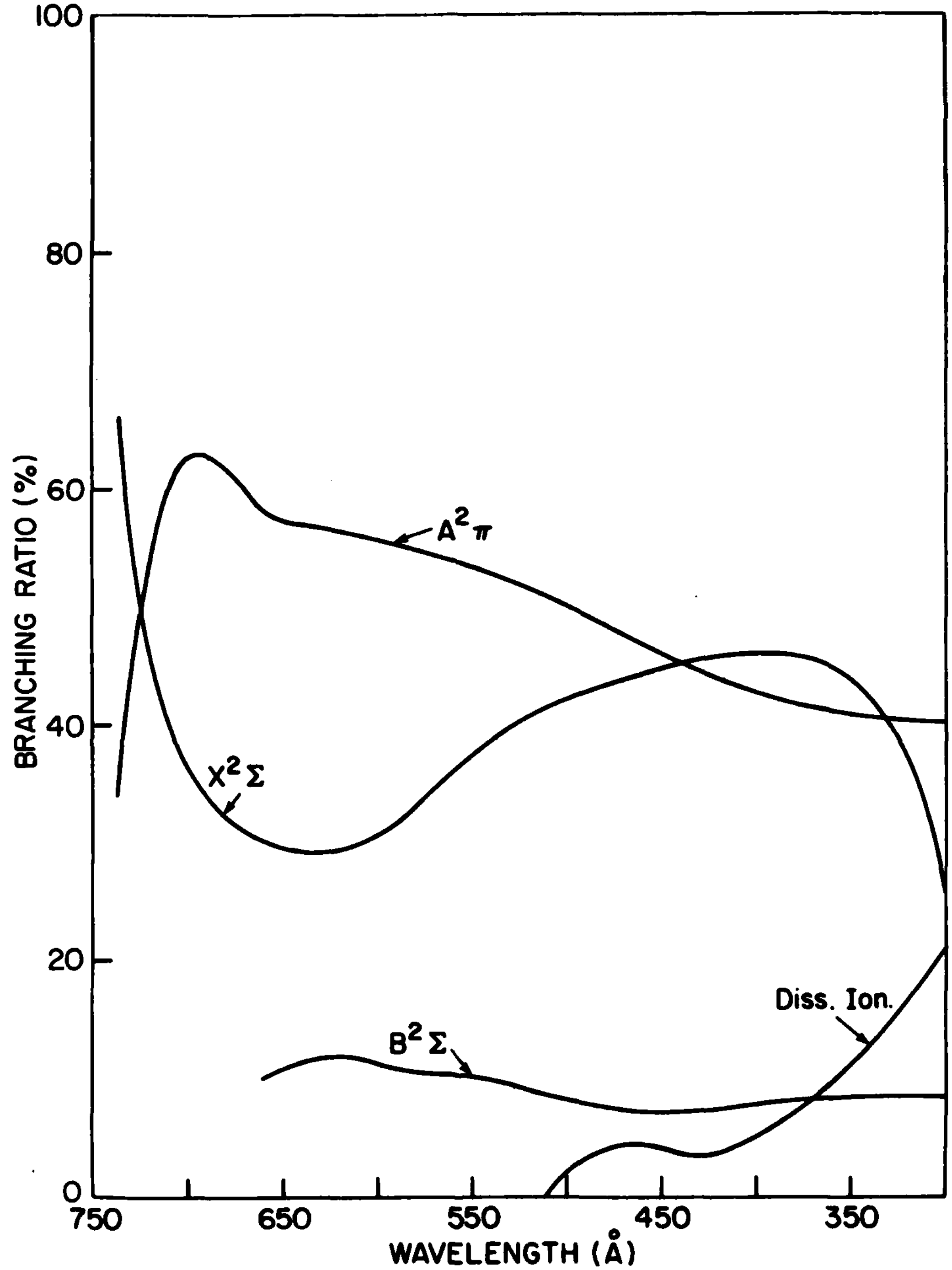

Fig. 1 - Branching ratio of various photoionization continue of N_2 as a function of the wavelength of the incident radiation

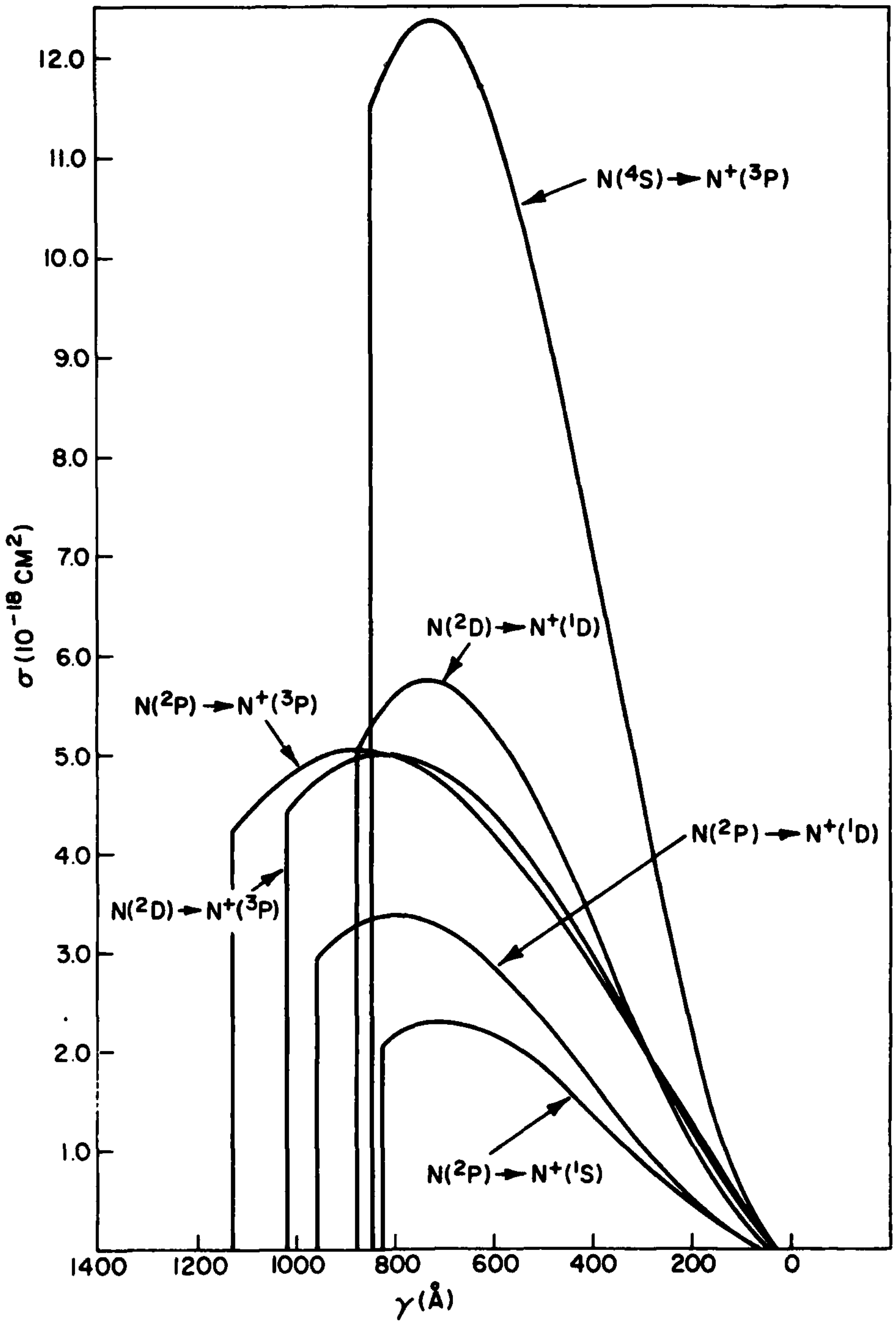

Fig. 2 - Photoionization cross sections for the ground state configurations of nitrogen atom

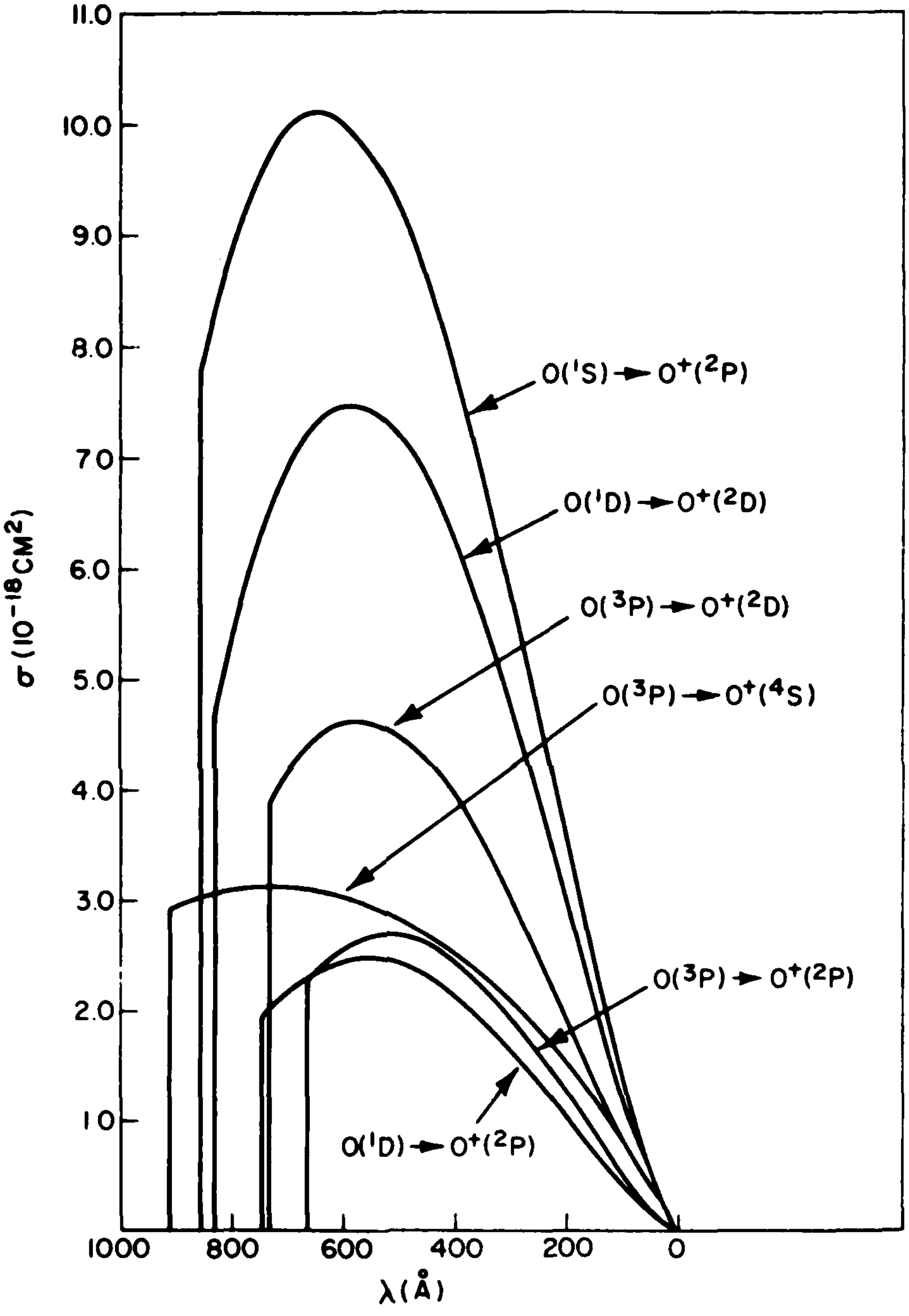

Fig. 3 - Photoionization cross section for the ground state configurations of the oxygen atom

MED

8